Optics Letters

Label-free plasmonic assisted optical trapping of single DNA molecules

Lei Chen,[1,2,6] Wei Liu,[3] Dongyi Shen,[3] Zhihao Zhou,[4] Yuehan Liu,[5] and Wenjie Wan[3,4,*]

[1]School of Physics and Optoelectronic Engineering, Foshan University, Foshan 528000, China
[2]Guangdong-Hong Kong-Macao Joint Laboratory for Intelligent Micro-Nano Optoelectronic Technology, Foshan University, Foshan 528225, China
[3]The State Key Laboratory of Advanced Optical Communication Systems and Networks, Department of Physics and Astronomy, Shanghai Jiao Tong University, Shanghai 200240, China
[4]MOE Key Laboratory for Laser Plasmas and Collaborative Innovation Center of IFSA, The University of Michigan-Shanghai Jiao Tong University Joint Institute, Shanghai Jiao Tong University, Shanghai 200240, China
[5]Whiting School of Engineering, Johns Hopkins University, Baltimore, Maryland 21218, USA
[6]e-mail: leichen_1990@126.com
*Corresponding author: wenjie.wan@sjtu.edu.cn

Received 28 January 2021; revised 19 February 2021; accepted 20 February 2021; posted 22 February 2021 (Doc. ID 420957); published 15 March 2021

DNA molecules are hard to catch using traditional optical trapping due to the nanometer width of their chains. Here we experimentally demonstrate a label-free optical trapping of a single micrometer λ-DNA in solution by the aid of plasmonic gold nanoparticles (GNPs), where a double-laser trap induces strong optical interparticle forces for the tweezer. We examine such sub-resolved interparticle forces by tracking the GNP dynamics in solution. Moreover, surface-enhanced Raman scattering signals of trapped λ-DNA have also been measured simultaneously in the same setup. In comparison with prior works, ours benefit from the excitation in a dynamic configuration without fabrication. This technique opens a new avenue for all-optical manipulation of biomolecules, as well as ultra-sensitive bio-medical sensing applications.

https://doi.org/10.1364/OL.420957

Optical tweezer/trapping technology has emerged as a prime tool for biological research over the last three decades, ever since the pioneering works by Ashkin and co-authors [1,2]. However, biomolecule form factors such as size and shape greatly lower the trapping efficiency of optical tweezers [3], which are mainly based on an optical gradient force in the limit of a diffraction spot. Specifically, for single DNA molecule trapping, traditional trapping techniques encounter problems mainly due to the nanoscale size and irregular chain-like shapes of these molecules. So far, many studies have been made on DNA in which it is stretched or transported by attaching DNA to a polystyrene bead and using an optical tweezer to exert force on the bead [4]. Although this optical technique has often been used in recent biophysical studies, chemical modification of the chain end is almost unavoidable [4,5], such that biophysical properties of DNAs are studied through indirect manipulation. Meanwhile, direct DNA trapping is also possible with designed electrodes according to the dielectrophoresis effect [6,7], but involving complicated microfabrication.

With the aid of plasmonic structures, optical trapping has successfully demonstrated the possibility of single molecule trapping in a label-free manner [8]. Similarly, several improved methods have been proposed to enhance the electromagnetic field of light, including the use of near-field optical devices such as slot waveguides [9], whispering-gallery mode resonators [10], and photonic crystals [11]. However, plasmonic trapping techniques based on surface plasmon polaritons (an electromagnetic excitation existing on the surface of a good metal) not only can enhance trapping, but also can serve as biosensors through nonlinear surface-enhanced Raman scattering (SERS) [8]. So far, most of these composite nanostructures are permanent structures, via nanofabrication or nanoparticle self-assembly [12,13]. Recently, controlled metallic nano-aggregations in solution offer a convenient and lower-fabrication alternative with single molecule sensitivity [14]. This technique may pave a new way for trapping and sensing biomolecules in an all-optical fashion.

In this Letter, based on our previous work [14], we experimentally demonstrate label-free optical trapping of a single micrometer-scale λ-DNA molecule in solution with the aid of plasmonic GNPs, where a double-laser trap induces strong near-field optical interparticle forces for the tweezer. Furthermore, this induced optical force rising from strong localized plasmon resonance strongly affects the interparticle separation deep below the optical diffraction limit. We investigate indirectly such sub-resolved interparticle forces in trapped nano-aggregates by analyzing the particle motion in liquid, which is more intuitive and convenient than the previous spectroscopic method based on SERS monitoring [14]. Meanwhile, the SERS spectra of trapped DNA molecule is revealed simultaneously based on the current trapping scheme. Although several special optical tweezers rely on metallic

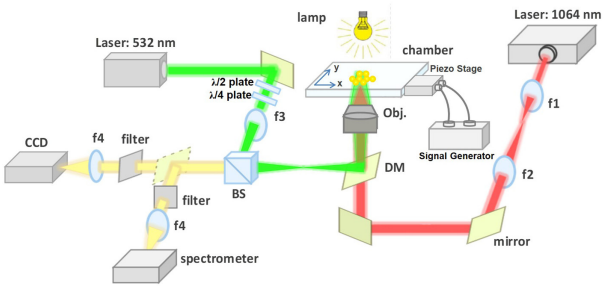

Fig. 1. Schematic of the double-laser trapping scheme. The signal generator is used to modulate the oscillation frequency of the cuvette through the piezo stage. The beam telescope sends the laser to slightly overfill the back aperture of the high-NA (1.25) trapping objective. The trapping and aggregation are observed with a charge-coupled device (CCD) camera, and SERS spectra are collected by a commercial spectrometer. The lamp on the right top is used for imaging.

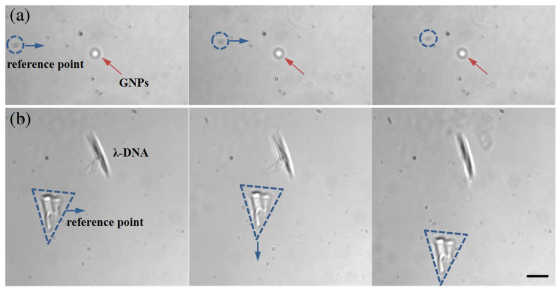

Fig. 2. Optical micrographs of trapping behavior of (a) GNPs and (b) λ-DNA recorded using a CCD camera. The length of the scale bar (black line in the lower right corner) is 3 μm. The blue arrows indicate the direction of reference point motion. The red arrows indicate the trapped GNPs.

nanostructures have confined biomolecules in a potential well, in practice these techniques suffer drawbacks such as high precision requirements in fabrication and fixed-trapping regions. By contrast, our technique circumvents the need of fabricating the required and usually permanent plasmonic nanostructures and architectures (e.g., tips, nanoholes, and metallic assemblies) [15–17] for DNA trapping and manipulation. This new technique enables new possibilities for all-optical manipulation of biomolecules, as well as ultra-sensitive bio-chemical sensing applications.

Figure 1 shows optical trapping of a single DNA molecule assisted by GNPs in a double-laser trap experimental apparatus, where the first laser from a 1064 nm continuous-wave fiber laser (NKT Photonics, Y10) acts as a "macroscopic" trap to confine GNPs in its focus region; in the meantime, a 532 nm green laser is used to induce the interparticle interactions when particles are in close proximity. The gold nanoparticles (GNPs) used are spherical with an average diameter of 20 nm. A lens f3 ($f = 60$ mm) is used to separate the focal plane of 532 and 1064 nm lasers; thereby, the 532 nm laser is loosely focused in the trapping spot to avoid possible photo-thermal damage. The power of the incident laser at the sample is 100 mW; the sample is usually located 2–3 μm below the focal plane of the high-NA objective lens, giving the actual laser intensity 2 mW/μm^2, at which the photo-thermal effect is negligible during the experiments. More details of the experimental setup and sample preparation are given in Supplement 1. Consequently, hot spots inside a trapped GNP greatly reduce their average spacing (<10 nm) due to a strong attractive force [14], acting as a tweezer tunable by laser illumination. Such an optical tweezer is perfectly suitable for trapping molecules such as DNA, which has a width ∼1 nm, but a length of over a micrometer. Unlike previous methods, this trapping scheme is capable of manipulating a single DNA molecule without the need for a label as in DNA-bead complex techniques and further benefits from the excitation in a solution without rigid fabrications. Here the optical interparticle forces play a crucial role for the nanometer interparticle spacing which is important not only for trapping long-chain DNA in this Letter, but also may create a strong gradient force for smaller molecules.

Figure 2 demonstrates the trapping process for the single DNA molecule using our technique. First, a 1064 nm laser is switched on to trap GNPs in the focus region, where GNPs gather in the center of the focal spot and form nano-aggregates. To confirm that the GNRs are stably trapped, Fig. 2(a) exhibits the dynamic trapping process of GNPs when the cuvette moves along the horizontal direction. As can be seen, the trapped GNPs firmly stay in the same position, while the position of the reference point moves along with the piezoelectric stage. The number of trapped particles is estimated through the single particle counting [18], according to the video recording (see Visualization 3). Note that the laser intensity (100 mW) used here is insufficient to trap and manipulate DNA directly under the conventional optical tweezer setup. As a result, the DNA molecule cannot be trapped directly with a sole 1064 nm trap due to the large average spacing between trapped GNPs. Sequentially, we introduce a secondary 532 nm laser to encourage interparticle attraction forces in order to shrink gap spacing between GNPs for DNA trapping. As soon as we turn on the 532 nm laser combined with the 1064 nm laser, a single DNA is observed to be trapped. Figure 2(b) shows a series of optical micrographs of representative DNA trapping behavior under double-laser illuminations. The molecule used is double-stranded λ-DNA (48.5 kbp) with sample concentrations of 0.3 μg/μl. When moving the sample cuvette, the reference point moves along with it, while the trapped λ-DNA stays in the same place, which indicates that the λ-DNA can be stably trapped in this plasmonic trapping system. The location of the trapped GNPs with respect to the DNA molecule is illustrated intuitively in Fig. S1. The direct evidence of sequential data is given in Visualization 1 and Visualization 2.

Here the induced interparticle forces are strongly influenced by the interparticle separation deep below the optical diffraction limit; this further affects the trapping efficiency on DNA molecules. Previously, we adapt an SERS signal measurement to estimate such nanometer gap separation [14]. Here we indirectly examine such sub-resolved interparticle forces in trapped GNPs in a mechanical way by tracking the GNP motion in the solution in order to evaluate the trapping efficiency of DNA. An external driving force (F_d) exerts on the particles through a piezo-driven stage by a signal generator (see Fig. 1). The attractive optical force (F_{opt}) glue trapped GNPs together against the external driving force, i.e., when $F_{\text{opt}} < F_d$, the trapped GNPs fall apart. We can approximate the total optical force as the sum of two terms $F_{\text{opt}} = F_{\text{inter}} + F_{\text{trap}}$ due to the interparticle coupling and the other associated with trapping, respectively. Since the driving force arising from the friction between GNPs and the solution which can be controlled by the oscillation

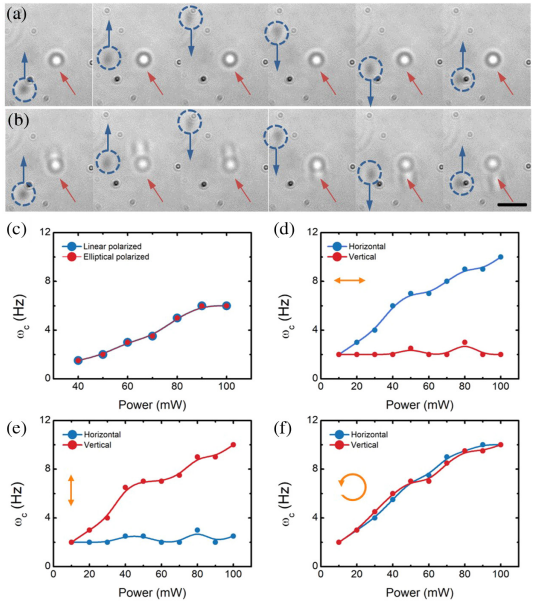

Fig. 3. (a), (b) Successive images of trapping process of GNPs recorded using a CCD camera when the oscillation frequency is below (a) and reaches (b) a critical frequency ω_c. The image sequence is from left to right with a time interval between images of 0.04 s. The dotted circle indicates the reference point. The blue arrow indicates the reference point moving direction. The red arrows indicate the trapped GNPs. The length of the scale bar (black line in the lower right corner) is 3 μm. (c) Critical frequency as a function of 1064 nm laser power at polarized and elliptical polarized excitation. (d)–(f) Critical frequency as a function of 532 nm laser power, as the polarization of a 532 nm laser varies along the motion direction parallel to the driving force and perpendicularly and elliptically. The insets donate the polarization of the 532 nm laser.

frequency (ω) of the cuvette driven by the piezo stage, we can evaluate the optical force magnitude by modulating the driving force.

Figures 3(a) and 3(b) show the dynamic trapping process of GNPs when the oscillation frequency is below [Fig. 2(a)] and reach a critical frequency (ω_c) [Fig. 2(b)], which represent the balance point of $F_{opt} = F_d$. Clearly, the trapped GNPs remain a perfect circle in the entire trapping process indicating a stable trapping as shown in Fig. 2(a). In contrast, the trapped GNPs fall apart in a comet-like tail when they reach the critical frequency [Fig. 2(b)], because the interparticle forces between GNPs cannot resist the driving force to keep steady trapping. Furthermore, the GNPs can fall apart or even float away at a higher frequency.

In our experiment, the trap stiffness of GNPs can be altered dynamically by modulating the light intensity. To investigate the interparticle forces inside GNPs, we exam critical frequency (ω_c) variation with respect to trapping laser power. First, we explore the "macroscopic" trap force with sole 1064 nm. Figure 3(c) shows laser power-dependent of the critical frequency with the 1064 nm trap. Here the incident power of a 1064 nm laser range from 40 to 100 mW, keeping both the driving force and laser polarization along the horizontal direction. As can be seen, the critical frequency varies from 1.5 to 6 Hz by increasing the laser power and saturates at 90 mW. To exam the polarization influence of the 1064 nm laser on the results similar to prior work [14], we compare the critical frequencies of linear polarization and elliptical polarization. Obviously, the polarization state of the 1064 nm laser can hardly influence the results, which clearly indicates the main role for such a "macroscopic" trapping laser without interfering GNP interparticle interaction.

As soon as we turn on the 532 nm laser trap simultaneously [Fig. 3(d)], the interparticle force is induced to reinforce the whole GNP package. Here the 1064 nm laser power is fixed at 50 mW; the polarization of the 532 nm laser varies along the motion direction parallel to the driving force (blue dots) and perpendicularly (red dots). As a result, the critical frequency increases compared to Fig. 3(c) (2 Hz), one major contribution arises from the induced interparticle attractive forces among GNPs. Similarly, the critical frequency increases from 2 to 10 Hz when increasing the incident power of the 532 nm laser with a parallel polarization to the motion direction, whereas the critical frequency remains almost constant (2 Hz) when the driving force is perpendicular to the 532 nm laser polarization in Fig. 3(d). This indicates that the induced interaction is sensitive to the 532 nm laser polarization, where GNPs may be attracted by interparticle forces and form nano-aggregates along with the polarization. To be more persuasive, we also verify the same results when altering the motion direction as shown in Fig. 3(e). On the other hand, for the elliptical polarized case in Fig. 3(f), the critical frequency exhibits almost the same trend independent of the driving force direction, which is an outcome of the two-dimensional axial symmetry of the interparticle forces induced by the elliptical polarized laser. This method provides us another important way to investigate the interparticle interactions inside GNPs in the micro-scale below the diffraction limit.

We also estimate the total force exerted on the particle from experimental particle movements following Ref. [19] (Fig. 4). The analytical procedure is based on $F_{opt} = m\dot{v} + F_d$, where v is the acceleration of the particle. The velocity v and acceleration $\dot{v}$ for the particle dynamics can be extracted from the videos captured using the CCD camera. The driving force exerted on particles in solution can be calculated from $F_d = \mu v$ with drag coefficient $\mu = 6\pi\eta a$, where η is the viscosity of water and a particle radius. The temperature distribution in the focused plasmonic tweezers system at different incident laser intensities is experimentally examined in Fig. S2, which shows that the maximum temperature increase of GNPs at an incident laser intensity is only about 5 K. This value for the laser-induced heating is comparable to the values measured before [16]. It should be noted that such a photothermal effect hardly induces thermal denaturation of DNA, because the elevated temperature is lower than the DNA melting point (99°C) [20]. Since the thermal temperature shows a negligible change with laser power, we take the viscosity of water as a constant of 0.7, which may result in deviations in these estimations. It can be seen that the force reaches the level of tens of piconewtons which almost equals the magnitude of the force required to stretch DNA (typically ~ 25 pN) [21]. Therefore, we expect that this technique may offer an alternative method for these DNA biophysics studies in the near future.

Based on the above double-laser trap scheme, we also perform a simple method for λ-DNA detection based on SERS signals, since metal nanostructures can produce great electromagnetic field enhancement, which is the main contribution of SERS. A typical SERS spectrum measured from a trapped λ-DNA molecule using our two-color excitation setup is given in Fig. 5.

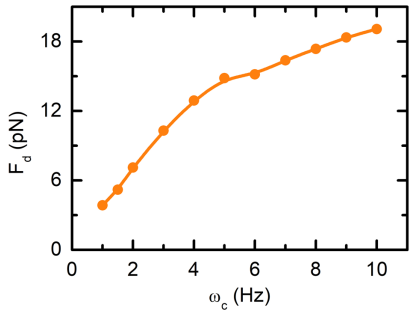

Fig. 4. Estimated driving force (F_d) exerted on GNPs at different output frequencies.

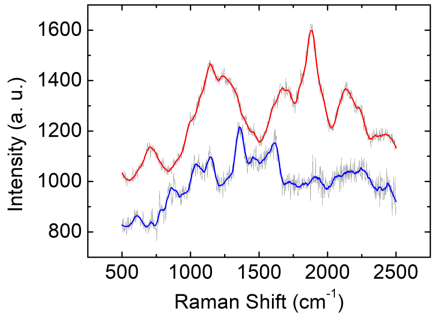

Fig. 5. Spectrum (top plot) from a typical SERS measurement of a single DNA molecule plotted against a background spectrum (bottom plot). The raw data (gray line) are plotted with their smoothed counterparts (Savitzky–Galey, 30 points) for both the DNA (top plot) and background (bottom plot) spectra and are shifted for clarity. The SERS detection is conducted using our experimental setup in Fig. 1 under 523 nm laser excitation. The laser intensity of 532 nm is 2.5×10^5 W/cm^2. The Integration time is 5 s.

The spectrum shown in gray is plotted directly from the spectrometer, without any smoothing or background removal. A background curve was also measured, at the same conditions, with the DNA moved away from the trap until the signal disappeared from the short time live scans. The SERS peaks at 712 and 1143 cm^{-1} in Fig. 5 are consistent with previous reports [22], while the peaks centered at 1877 cm^{-1} is shifted to a higher wavenumber. This shift of Raman frequencies might indicate the different stretching states of DNA molecules which probably influence the Raman frequencies. Combined with the above molecule trapping, we can expect that the current technique offers a new way for single molecule trapping and sensing simultaneously in bio-medical applications.

In summary, we experimentally demonstrate label-free optical trapping of λ-DNA in solution assisted by plasmonic GNPs in a double-laser trap with SERS sensing capability. This technique can also be used to manipulate other biomolecules such as nucleic acids, proteins, and polysaccharides and will prove to be a useful tool in the application of biosensors. Our experiment has yet to be expanded, as in most cases, all nanoparticles are trapped and aggregated in the center of the potential well, producing chaos and disorder that leads to non-uniform and unpredictable enhancement factors in the nano-gaps. In future work, we will investigate methods to accurately control the number of nano-gaps and explore the potential for ultrahigh spatial resolution SERS imaging.

Funding. Research Fund of Guangdong-Hong Kong-Macao Joint Laboratory for Intelligent Micro-Nano Optoelectronic Technology (2020B1212030010); Shanghai MEC Scientific Innovation Program (E00075); National Natural Science Foundation of China (92050113); National Key Research and Development Program of China (2016YFA0302500).

Disclosures. The authors declare no conflicts of interest.

Supplemental document. See Supplement 1 for supporting content.

REFERENCES

1. A. Ashkin, J. M. Dziedzic, J. E. Bjorkholm, and S. Chu, Opt. Lett. **11**, 288 (1986).
2. A. Ashkin and J. M. Dziedzic, Science **235**, 1517 (1987).
3. Y. Tsuboi, T. Shoji, M. Nishino, S. Masuda, K. Ishimori, and N. Kitamur, Appl. Surf. Sci. **255**, 9906 (2009).
4. I. Heller, T. P. Hoekstra, G. A. King, E. J. G. Peterman, and G. J. L. Wuite, Chem. Rev. **114**, 3087 (2014).
5. G. V. Shivashankar, M. Feingold, O. Krichevsky, and A. Libchaber, Proc. Natl. Acad. Sci. USA **96**, 7916 (1999).
6. L. Ulanovsky, G. Drouin, and W. Gilbert, Nature **343**, 190 (1990).
7. C. L. Asbury, A. H. Diercks, and G. van den Engh, Electrophoresis **23**, 2658 (2002).
8. J. Shen, J. Wang, C. Zhang, C. Min, H. Fang, L. Du, S. Zhu, and X. C. Yuan, Appl. Phys. Lett. **103**, 191119 (2013).
9. A. H. J. Yang, S. D. Moore, B. S. Schmidt, M. Klug, M. Lipson, and D. Erickson, Nature **457**, 71 (2009).
10. S. Lin, E. Schonbrun, and K. Crozier, Nano Lett. **10**, 2408 (2010).
11. Y.-F. Chen, X. Serey, R. Sarkar, P. Chen, and D. Erickson, Nano Lett. **12**, 1633 (2012).
12. L. Gunnarsson, E. J. Bjerneld, H. Xu, S. Petronis, B. Kasemo, and M. Käll, Appl. Phys. Lett. **78**, 802 (2001).
13. L. Polavarapu and Q.-H. Xu, Langmuir **24**, 10608 (2008).
14. L. Chen, W. Liu, D. Shen, Y. Liu, Z. Zhou, X. Liang, and W. Wan, Nanoscale **11**, 13558 (2019).
15. Y. Pang and R. Gordon, Nano Lett. **11**, 3763 (2011).
16. T. Shoji, J. Saitoh, N. Kitamura, F. Nagasawa, K. Murakoshi, H. Yamauchi, S. Ito, H. Miyasaka, H. Ishihara, and Y. Tsuboi, J. Am. Chem. Soc. **135**, 6643 (2013).
17. K. Jung-Dae and L. Yong-Gu, Biomed. Opt. Express **5**, 2471 (2014).
18. C. Hosokawa, H. Yoshikawa, and H. Masuhara, Phys. Rev. E **72**, 021408 (2005).
19. M. Ichikawa, Y. Matsuzawa, Y. Koyama, and K. Yoshikawa, Langmuir **19**, 5444 (2003).
20. M. C. Williams, J. R. Wenner, I. Rouzina, and V. A. Bloomfield, Biophys. J. **80**, 1932 (2001).
21. M. D. Wang, H. Yin, R. Landick, J. Gelles, and S. M. Block, Biophys. J. **72**, 1335 (1997).
22. H. Wei and H. Xu, Appl. Phys. A **89**, 273 (2007).